Delft University of Technology

Using Fiber Bragg Grating Sensors to Quantify Temperature Non-Uniformities in Plasmonic Catalyst Beds under Illumination

Xu, Man; den Hartog, Tim; Cheng, Lun; Wolfs, Marciano; Habets, Roberto; Rohlfs, Jelle; van den Ham, Jonathan; Meulendijks, Nicole; Sastre, Francesc; Buskens, Pascal
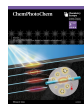
Important note
To cite this publication, please use the final published version (if applicable).
Please check the document version above.

ChemPhotoChem

Research Articles
doi.org/10.1002/cptc.202100289

Chemistry
Europe

European Chemical
Societies Publishing

www.chemphotochem.org

Using Fiber Bragg Grating Sensors to Quantify Temperature Non-Uniformities in Plasmonic Catalyst Beds under Illumination

Man Xu,*[a, b] Tim den Hartog,[a, c] Lun Cheng,[a] Marciano Wolfs,[a, c] Roberto Habets,[a] Jelle Rohlfs,[a] Jonathan van den Ham,[a] Nicole Meulendijks,[a] Francesc Sastre,[a] and Pascal Buskens*[a, d]

Distinguishing between photothermal and non-thermal contributions is essential in plasmon catalysis. Use of a tailored optical temperature sensor based on fiber Bragg gratings enabled us to obtain an accurate temperature map of an illuminated plasmonic catalyst bed with high spatiotemporal resolution. Its importance for quantification of the photothermal and non-thermal contributions to plasmon catalysis is demonstrated using a Ru/Al$_2$O$_3$ catalyst. Upon illumination with LEDs, we measured temperature differences exceeding 50 °C in the top 0.5 mm of the catalyst bed. Furthermore, we discovered differences between the surface temperature and the temperature obtained via conventional thermocouple measurements underneath the catalyst bed exceeding 200 °C at 2.6 W cm^{-2} light intensity. This demonstrates that accurate multi-point temperature measurements are a prerequisite for a correct interpretation of catalysis results of light-powered chemical reactions obtained with plasmonic catalysts.

Introduction

The direct use of (sun)light as sustainable energy source for powering chemical reactions can become an important contributor to the transition from the current fossil-based chemical industry to a climate neutral one.[1] A technology concept that facilitates the direct use of light for chemical processes is plasmon catalysis.[2] In plasmon catalysis, the localized surface plasmon resonance (LSPR) of metallic nanocatalysts is essential.[3] Illumination with light triggers a coherent electron oscillation in the catalyst particles, which de-phases and generates hot electrons. These can contribute to chemical reactions in two ways: they can be injected into unoccupied molecular orbitals of reactants adsorbed on the surface of the metal nanocatalyst (non-thermal contribution), and they can thermalize to a Fermi-Dirac distribution via electron-electron and electron-phonon scattering, resulting in an increased temperature of the catalyst (photothermal contribution).[4]

Distinguishing between photothermal and non-thermal contributions is essential in plasmon catalysis, both from a fundamental and application perspective. Multiple research groups are currently focusing their investigations on this subject matter for various reactions and catalysts. Halas, Nordlander and co-workers attempted to quantify the photothermal and hot carrier contributions for the decomposition of NH$_3$ into H$_2$ and N$_2$ using a plasmonic Cu–Ru nanocatalyst.[5] They determined the reaction rate for a range of different wavelengths and light intensities, and claimed that the activation energy of this reaction depends on the wavelength and intensity of the light that is used to power it. They introduced the concept of a light-dependent activation barrier to account for the effect of light illumination on electronic and thermal excitations in one comprehensive picture. Li and co-workers reported a method for distinguishing between thermal and non-thermal contributions by measuring the top and bottom temperature of the catalyst bed using two thermocouples.[6] For the LED-powered Rh/TiO$_2$ catalysed conversion of CO$_2$ and H$_2$ to CH$_4$ the authors claimed that their method – together with a study of the reaction rate in dark at various temperatures – allowed them to distinguish between the thermal and non-thermal contributions, assuming a linear temperature gradient in the catalyst bed. They reported substantial non-thermal

[a] Dr. M. Xu, Dr. T. den Hartog, L. Cheng, M. Wolfs, R. Habets, J. Rohlfs, Dr. J. van den Ham, N. Meulendijks, Dr. F. Sastre, Prof. Dr. P. Buskens
The Netherlands Organisation for Applied Scientific Research (TNO)
High Tech Campus 25
5656AE Eindhoven (The Netherlands)
E-mail: man.xu@tno.nl
pascal.buskens@tno.nl

[b] Dr. M. Xu
Optics Research Group
Delft University of Technology
Lorentzweg 1 (Building 22)
2628CJ Delft (The Netherlands)

[c] Dr. T. den Hartog, M. Wolfs
Zuyd University of Applied Sciences
Nieuw Eyckholt 300
6400AN Heerlen (The Netherlands)

[d] Prof. Dr. P. Buskens
Institute for Materials Research
Design and Synthesis of Inorganic Materials (DESINe)
Hasselt University
Agoralaan Building D, 3590 Diepenbeek (Belgium)

ChemPhotoChem

Research Articles
doi.org/10.1002/cptc.202100289

**Chemistry
Europe**
European Chemical
Societies Publishing

contributions, expressed by an apparent quantum efficiency of up to 46%. Furthermore, they claim that heat and light works synergistically in their process with increasing non-thermal contributions at higher temperatures.

Recently, Baffou et al. reviewed[7] and proposed a series of experiments that can contribute to distinguishing between photothermal and non-thermal effects in plasmon catalysis. This includes varying the illumination power. When varying the illumination power, reactions initiated via an injection of hot electrons into antibonding orbitals of adsorbed reactants show a linear dependence on the irradiance for moderate light power and continuous wave illumination, since the rate of the molecular transformations is proportional to the rate of photons. Since the temperature of the catalyst is proportional to the light absorption and rate constants of chemical reactions typically follow an Arrhenius-type of temperature dependence, photothermal reactions display an exponential relationship between the reaction rate and the irradiance. Furthermore, Baffou et al. explain that when the illumination spot size is much larger than the distance between two particles – which is typically the case in plasmon catalysis – the illumination of a large number of particles at the same time gives rise to collective thermal effects, effectively suppressing nanoscale temperature inhomogeneities and leading to a macroscopically homogeneous temperature distribution. Based on this, they suggest that accurate macroscopic temperature measurements – taking into account temperature profiles in x,y- and gradients in z-direction of the catalyst bed – are the key to quantifying photothermal and non-thermal contributions. Temperature gradients from top to bottom of the catalyst bed upon illumination are due to gradual extinction of light, and have an impact on the activity of the catalyst (Arrhenius law). Furthermore, they may also impact the product selectivity. This is confirmed by Sivan and Dubi,[8] who stated that "as long as temperature gradients exist inside the system (as for typical experimental setups) a quantification of non-thermal effects is close to impossible."

When temperature measurements of the catalyst bed are performed, to date mostly thermocouples or/and infrared (IR) cameras are used.[6,9] However, thermocouples do not suffice for this purpose. They cannot be used for temperature measurements at or close to the top surface of the catalyst bed, since direct exposure of the thermocouple to light would lead to an overestimation of the catalyst temperature due to the direct light absorption by the thermocouple. Furthermore, using multiple thermocouples in a catalyst bed would result in a relatively large mass of the thermocouples when compared to the amount of catalyst, which means that a substantial part of the photothermal energy of plasmon catalysis would go into heating of the thermocouples leading to an underestimation of its contribution. Additionally, a good thermal contact between the typically millimetres thick thermocouple and the catalyst is difficult to ensure, since the catalyst bed is merely loosely packed. Improper thermal contact can easily lead to a large underestimation of the catalyst bed temperature, and addition of materials that improve this thermal contact could influence the thermal characteristics of the catalyst and the catalytic

process, when using the temperature measurement *in operando*. Temperature measurements based on infrared thermal cameras are also insufficient. Using an IR camera, the surface temperature of the catalyst bed can be imaged, giving insight into temperature differences in the x,y-plane. However, they don't yield any information on the temperature gradient in the z-direction.[9b] Furthermore, obtaining accurate temperature values from an infrared thermal camera requires detailed information on the emissivity of the plasmonic catalysts, which is not simply available and takes extra effort to measure and obtain.

Here, we report the development of a fiber Bragg grating (FBG)-based fiber optic sensor (FOS),[10] which is much smaller than conventional thermocouples, has a much lower mass and does not directly absorb light. This FBG-based method overcomes all limitations[11] reported above for temperature measurements using thermocouples and/or infrared thermal cameras. We demonstrate that this FOS enables accurate temperature measurements at multiple positions inside an illuminated plasmonic catalyst bed enabling monitoring of local temperatures and temperature profiles and gradients.

Results and Discussion

We validate the performance of this FOS sensor using spherical and rod-like alumina-supported Ru nanocatalysts recently developed by our research group for sunlight-powered conversion of CO_2 and H_2 to CH_4.[12] For the image of the sample, we refer to our previous publication.[12b] The inspection of the NPs using TEM can be seen in S2. Using the FOS, we measured temperature differences exceeding 50 °C in the top 0.5 mm of the catalyst bed. Furthermore, we discovered differences between the surface temperature and the temperature obtained via conventional thermocouple measurements underneath the catalyst bed exceeding 200 °C. This demonstrates that accurate multi-point temperature measurements are a prerequisite for a correct interpretation of catalysis results of light-powered chemical reactions obtained with plasmonic catalysts.

We have constructed a FBG-based FOS (see S5) to measure the temperature distribution inside a plasmonic catalyst bed. A copy of the sample holder used in our previous reports[12b] on the sunlight-powered Sabatier reaction is used as the fiber sensor mount. Figure 1b shows a metallic ring around a thin quartz filter. The catalyst is normally placed on top of this quartz filter, and illuminated from the top. The quartz filter, which in Figure 1b is not loaded with catalyst, is equipped with four 80 μm glass fibers to measure temperature at 4 different depths in the catalyst bed. For manufacturing and installation convenience, the 4 fibers placed at different depths are not mounted in a way that they overlap in z-direction, but are slightly displaced. Each fiber is levelled by 2 V-grooves carved in the ring at the designed depth. Due to the tiny size of the optical fiber, they cannot be seen clearly in picture. Therefore, 4 squares are marked on the fiber to indicate the location of the FBG-sensing points. The distance between the outmost two
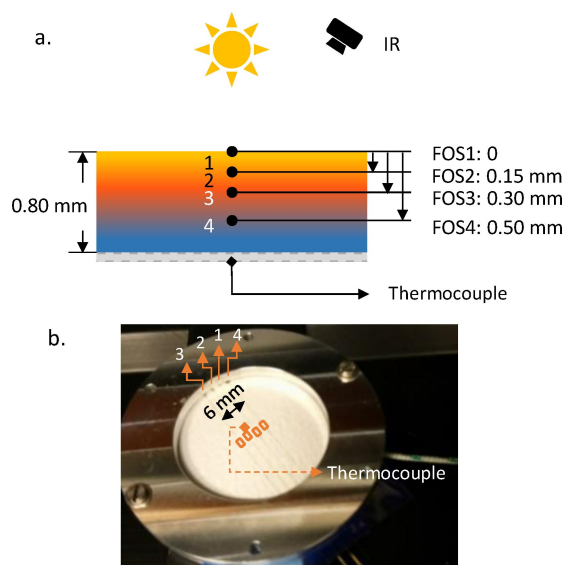
ChemPhotoChem

Research Articles
doi.org/10.1002/cptc.202100289

**Chemistry
Europe**
European Chemical
Societies Publishing

Figure 1. FBG-based FOS for temperature measurements in an illuminated plasmonic catalyst bed. (a) Schematic illustration and (b) FOS using FBG sensing unit mounted on a catalyst powder holder with a thermocouple attached underneath the catalyst bed.

Figure 2. (a) Temperature measurement by fiber optic sensors at four depths inside the catalyst bed as the LED is switched on and off; (b) Temperature changes as a function of light intensity; (c) The temperature gradient from the surface to 0.5 mm in the catalyst bed.

fibers is 0.6 mm. The corresponding depths for the 4 sensing points are shown in Figure 1a. The loosely packed black catalyst powder consisting of Ru nanoparticles on Al_2O_3 (see S1 for details of samples and characterization) with total thickness of 0.8 mm is later placed in a roughly 1 cm^2 square area in the center of the ring holder. The black NP powder samples have strong light absorption due to its morphology, as the light transmission through 0.5 mm thick NP powder becomes zero (see S4). FOS1 is positioned to measure the temperature at the very top position of the powder, and three other FOSs are placed up to a depth of 0.5 mm. We measure the temperature change in the catalyst bed under a homogeneous LED illumination covering the entire NP sample area in a reference non-reaction environment. Throughout experiments using our Ru/Al_2O_3 catalyst that has a broadband absorption in the visible range (see S3), we have found only minor influence of the illumination wavelength on the measured temperatures (see S7). Thus in this paper we exclusively present the results obtained with a blue LED with illumination wavelength centred at 445 nm (Full Width Half Maximum bandwidth of 23 nm). We have validated our temperature measurements by calibrating the FOS temperature response in a furnace, up to 200 °C (see S6). As a reference a thermocouple is placed in contact with the bottom of the NP holder to measure the temperature below the catalyst bed.

In a typical experiment using Ru nanospheres on Al_2O_3 (NS-1: 4.9 % Ru, 0.89 ± 0.15 nm diameter), illumination starts at t = 0 s by switching on the LED. The temperature increases quickly (equilibrium within 40 s in all experiments) from ambient temperature (Figure 2a). LED illumination is continued for 300 s and when the LED is switched off, a temperature drop follows quickly within the following minute. Eventually, ambient temperature is reached within 240 s in all experiments. The
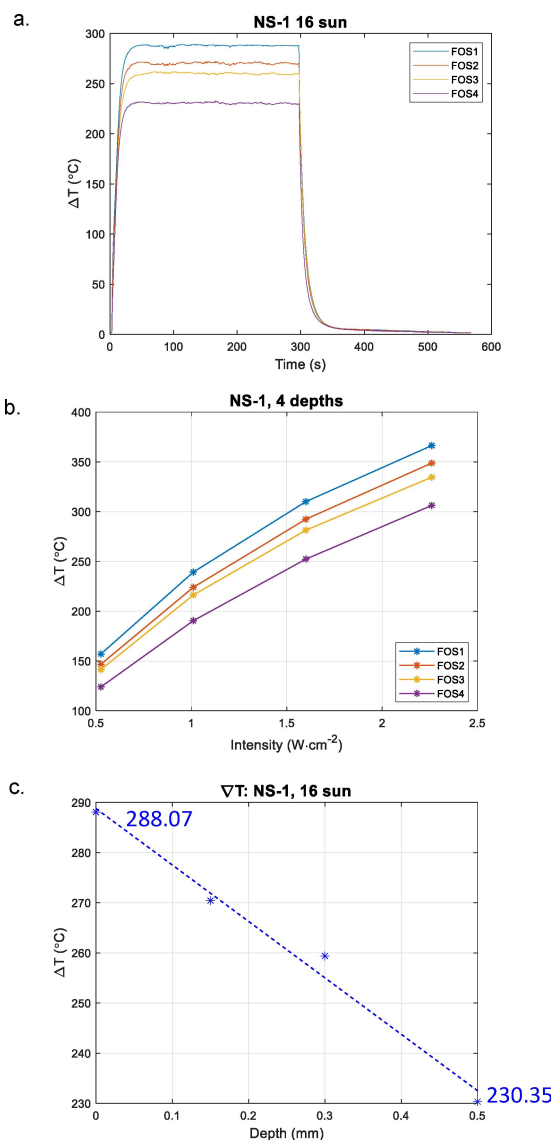
same time response has been observed for the different FOSs at different depths. We also observed that with various light intensities, the temperature increase follows at very similar rate. The temperature always stabilizes within 40 s. The temperature at thermal equilibrium is taken as the average temperature reading between 100 and 300 s. For light intensity varying from 0.50 W cm^{-2} to 2.26 W cm^{-2}, the temperature measured at the 4 depths from the surface to the body of the catalyst powder is shown in Figure 2b. For the 1.60 W cm^{-2} irradiance in the experiment in Figure 2a, the T gradient for the measured range can be fitted with a linear function (Figure 2c). The ΔT between the surface and at the depth of 0.5 mm in the catalyst powder bed is 58 °C, which gives a T gradient of 115 °C mm^{-1}.

Using the acquired information of the thermal gradient in the catalyst powders, we developed a simple empirical model to study the photothermal effect (see S8). In our model two

relevant heat transfer effects are counted: thermal radiation to the top space, and thermal conduction to the body of the catalyst bed. Using the FBG sensor system, we have fully characterized the temperature distribution of the catalyst bed upon light illumination. Using the model and the measurement data, the thermal conductivity is fitted (see S8). This is an indirect measurement method. Once the thermal conductivity is known, in the follow up research, the temperature sensory system can be simplified to 1-point measurement only needed at the bottom of the catalyst powder, assuming total thickness of catalyst material is around 1 mm. With the known light power input, the top layer temperature can be estimated using the equation derived in S8. Over a large temperature range, k has a small value between 0.04 to 0.08 $W\,m^{-1}\,K^{-1}$ which agrees with other reported value.[13] This low thermal conductivity is a result of nanoparticle morphology and it differs largely from their bulk counterparts' property. The same effect applies to other plasmon NP catalyst materials in general.

The surface temperature of 4 samples (sample description in S1) are measured. The measurement results and the fitted empirical model are plotted in Figure 3. Very little difference in surface temperature in the samples is observed, in spite of the different composition and varied particle size (see S1). The similar photothermal response reveals that the tested plasmonic catalysts in this paper have similar collective thermal properties even though the isolated single nanoparticles may display varied optical and thermal behaviours.[12b] For the tested large light intensity variation range, a nonlinear temperature increase of the catalyst material with the light power is observed. This nonlinear response can be explained by the nonlinearity of the thermal radiation function (according to the model described in S8). For a small light intensity variation range, the temperature response can appear to be linear and can be approximated using a linear function with the corresponding boundary values, as it has been done in one of our previous publication.[12c] Note: Our model does not include heat losses connected to the catalyst holder (via the quartz filter and the metal ring).

Most often thermocouples and/or IR cameras have been reported to measure the temperature of plasmonic catalysts.
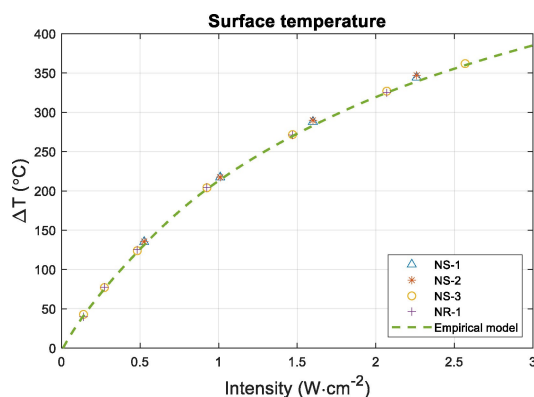
For comparison, we incorporated these techniques in our set-up and measured the catalyst temperature of Ru nanospheres on Al_2O_3 (NS-3: 6.4% Ru, 1.05±0.23 nm diameter) under LED light illumination (Figure 4). The thermocouple pushes up the filter surface under the NPs and lifts the lowest FBG position, FOS4 data is therefore omitted. At a light intensity of 0.925 $W\,cm^{-2}$, the measured T difference between the thermocouple and the FBG sensor at the top position (FOS1) is 118.55 °C. The difference is even larger at higher light intensity. We can conclude that the temperature is highly underestimated using a thermocouple, potentially leading to misinterpretations in the ratio between photothermal and nonthermal effects.

An incorrect emissivity setting of the IR camera leads to inaccurate reading in the temperature (see S9). To get accurate results for the surface temperature measurements using the IR camera the data were fitted to the top FBG sensor data to establish an estimated IR range emissivity – 0.95 in our case. In addition to the large temperature gradient in the z-direction established using the FBG sensor system, IR camera measurements identified a temperature variation in the x,y-plane. Depending on the sampling area, deviations in average
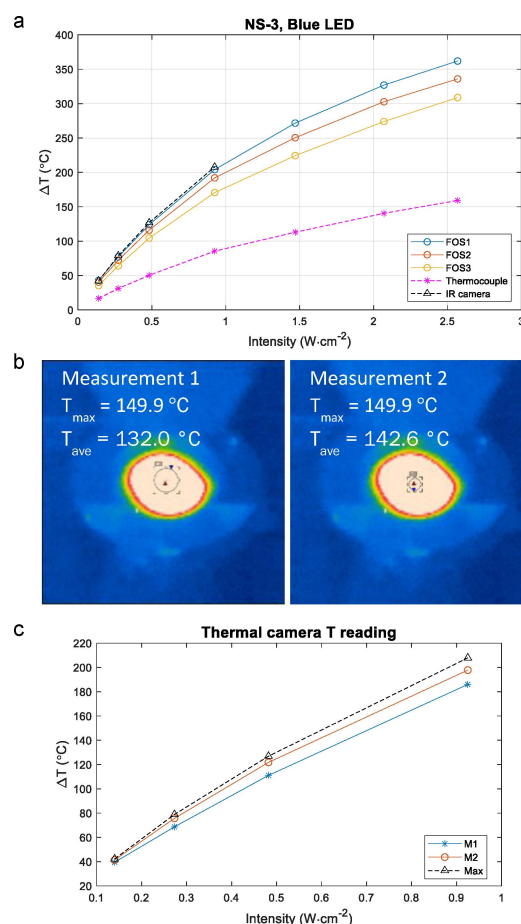

Figure 3. Surface temperature change measurements of 4 samples together with the fitted empirical model.

Figure 4. (a) Comparison of temperature measurements using FOS with a thermocouple and an IR camera; (b) Temperature reading by an IR camera with two sampling area sizes on the same image; (c) Three IR camera sampling methods result in different temperature values. Emissivity of the catalyst is 0.95.

ChemPhotoChem

Research Articles
doi.org/10.1002/cptc.202100289

Chemistry Europe
European Chemical
Societies Publishing

temperature were found (Figure 4b, 142.6 °C for smaller area vs. 132.0 °C for larger area). Thus, an IR camera can be used to accurately measure the surface temperature when establishing the correct emissivity of the plasmonic catalyst, and when a small area is sampled. However, an IR camera is unsuited to establish temperature gradients in the z-direction.

Conclusions

In conclusion, using a FBG sensor system we have been able to establish an accurate temperature map of a plasmonic catalyst powder bed upon illumination. We detected large temperature gradients in illuminated plasmonic catalyst powders (z-direction: 115 °C mm^{-1} at 1.6 W cm^{-2} light intensity). We have developed an empirical model, based on black body radiation and heat conduction. A low thermal conductivity of 0.04–0.08 W m^{-1}K^{-1} is found, which causes the large temperature non-uniformity in the NP catalyst bed and should be taken into account when distinguishing between thermal and non-thermal contribution to plasmon catalysis. A critical comparison of temperature measurements using the FBG sensor system and a thermocouple shows that the thermocouple measurements largely underestimate the temperature (up to 200 °C at 2.6 W cm^{-2} light intensity). When used and calibrated (emissivity) correctly an IR camera can be used to measure exclusively the surface temperature, and indicate a temperature variation in the x,y-direction. Further development of a FBG sensor system to map the catalyst temperature *in operando* is currently ongoing in our laboratories. We would also like to point out that the measured temperature gradients will lead to large local deviations in reaction rate, and possible access to additional reaction pathways and mixed reaction mechanisms. Latter may explain differences in selectivity between illuminated reactions and their counterparts in dark.

Conflict of Interest

The authors declare no conflict of interest.

Data Availability Statement

The data that support the findings of this study are available from the corresponding author upon reasonable request.

[1] International Renewable Energy Agency, **2020**, Report: Global Renewables Outlook: Energy transformation 2050, https://www.irena.org/publications/2020/Apr/Global-Renewables-Outlook-2020.

[2] a) G. Baffou, R. Quidant, *Chem. Soc. Rev.* **2014**, *43*, 3898–3907; b) P. G. O'Brien, A. Sandhel, T. E. Wood, A. A. Jelle, L. B. Hoch, D. D. Perovic, C. A. Mims, G. A. Ozin, *Adv. Sci.* **2014**, *1*, 1400001; c) F. Sastre, A. V. Puga, L. Liu, A. Corma, H. Garcia, *J. Am. Chem. Soc.* **2014**, *136*, 6798–6801; d) L. Zhou, C. Zhang, M. J. McClain, A. Manjavacas, C. M. Krauter, S. Tian, F. Berg, H. O. Everitt, E. A. Carter, P. Nordlander, N. J. Halas, *Nano Lett.* **2016**, *16*, 1478–1484; e) U. Aslam, V. G. Rao, S. Chavez, S. Linic, *Nat. Catal.* **2018**, *1*, 656–665; f) M. Verkaaik, R. Grote, N. Meulendijks, F. Sastre, B. M. Weckhuysen, P. Buskens, *ChemCatChem* **2019**, *11*, 4974–4980; g) A. Gellé, T. Jin, L. de la Garza, G. D. Price, L. V. Besteiro, A. Moores, *Chem. Rev.* **2020**, *120*, 986–1041; h) E. Cortés, L. V. Besteiro, A. Alabastri, A. Baldi, G. Tagliabue, A. Demetriadou, P. Narang, *ACS Nano* **2020**, *14*, 16202–16219; i) N. Blommaerts, N. Hoeven, D. Arenas Esteban, R. Campos, R. Mertens, R. Borah, A. Glisenti, K. De Wael, S. Bals, S. Lenaerts, S. W. Verbruggen, P. Cool, *Chem. Eng. J.* **2021**, *410*, 128234.

[3] a) F. Liebig, R. M. Sarhan, M. Bargheer, C. N. Z. Schmitt, A. H. Poghosyan, A. A. Shahinyan, J. Koetz, *RSC Adv.* **2020**, *10*, 8152–8160; b) R. F. Hamans, R. Kamarudheen, A. Baldi, *Nanomaterials* **2020**, *10*, 2377; c) C. D. Mendonça, S. U. Khan, V. Rahemi, S. W. Verbruggen, S. A. S. Machado, K. De Wael, *Electrochim. Acta* **2021**, *389*, 138734.

[4] a) L. Mascaretti, A. Naldoni, *J. Appl. Phys.* **2020**, *128*, 041101; b) D. Mateo, J. L. Cerrillo, S. Durini, J. Gascon, *Chem. Soc. Rev.* **2021**, *50*, 2173–2210; c) F. Zhang, Y.-H. Li, M.-Y. Qi, Y. M. A. Yamada, M. Anpo, Z.-R. Tang, Y.-J. Xu, *Chem. Catal.* **2021**, *1*, 272–297.

[5] L. Zhou, D. F. Swearer, C. Zhang, H. Robatjazi, H. Zhao, L. Henderson, L. Dong, P. Christopher, E. A. Carter, P. Nordlander, N. J. Halas, *Science* **2018**, *362*, 69–72.

[6] X. Li, X. Zhang, H. O. Everitt, J. Liu, *Nano Lett.* **2019**, *19*, 1706–1711.

[7] G. Baffou, I. Bordacchini, A. Baldi, R. Quidant, *Light-Sci. Appl.* **2020**, *9*, 108.

[8] a) Y. Sivan, J. Baraban, I. W. Un, Y. Dubi, *Science* **2019**, *364*; b) Y. Sivan, Y. Dubi, *Appl. Phys. Lett.* **2020**, *117*, 130501.

[9] a) X. Zhang, X. Li, M. E. Reish, D. Zhang, N. Q. Su, Y. Gutierrez, F. Moreno, W. Yang, H. O. Everitt, J. Liu, *Nano Lett.* **2018**, *18*, 1714–1723; b) R. Mutschler, E. Moioli, K. Zhao, L. Lombardo, E. Oveisi, A. Porta, L. Falbo, C. G. Visconti, L. Lietti, A. Züttel, *ACS Catal.* **2020**, *10*, 1721–1730; c) Y. Sivan, J. H. Baraban, Y. Dubi, *OSA Contin.* **2020**, *3*, 483–497.

[10] a) L.-K. Cheng, P. M. Toet, in *Opto-Mechanical Fiber Optic Sensors* (Ed.: H. Alemohammad), Butterworth-Heinemann, **2018**, 175–209; b) R. Kashyap, *Fiber Bragg Gratings*, 2nd ed., Academic Press, **2009**.

[11] T. Wei, X. Lan, H. Xiao, Y. Han, H. Tsai, in *2011 IEEE International Instrumentation and Measurement Technology Conference*, **2011**, 1–4.

[12] a) F. Sastre, C. Versluis, N. Meulendijks, J. Rodríguez-Fernández, J. Sweelssen, K. Elen, M. K. Van Bael, T. den Hartog, M. A. Verheijen, P. Buskens, *ACS Omega* **2019**, *4*, 7369–7377; b) R. Grote, R. Habets, J. Rohlfs, F. Sastre, N. Meulendijks, M. Xu, M. A. Verheijen, K. Elen, A. Hardy, M. K. Van Bael, T. den Hartog, P. Buskens, *ChemCatChem* **2020**, *12*, 5618–5622; c) P. Martínez Molina, N. Meulendijks, M. Xu, M. A. Verheijen, T. den Hartog, P. Buskens, F. Sastre, *ChemCatChem* **2021**, *13*, 1–8.

[13] a) W. Tian, R. Yang, *J. Appl. Phys.* **2007**, *101*, 054320; b) D. Tao, X. Li, Y. Dong, Y. Zhu, Y. Yuan, Q. Ni, Y. Fu, S. Fu, *Compos. Sci. Technol.* **2020**, *188*, 107992.